Journal of Polymer Research (2019) 26: 127
https://doi.org/10.1007/s10965-019-1784-7

ORIGINAL PAPER

Glycidyl methacrylate-based copolymers as new compatibilizers for polypropylene/ polyethylene terephthalate blends

Mafalda S. Lima[1] · Áurea A. Matias[1] · João R. C. Costa[1] · Ana C. Fonseca[1] · Jorge F. J. Coelho[1] · Arménio C. Serra[1]

Received: 5 February 2019 / Accepted: 9 April 2019 / Published online: 3 May 2019

Abstract

The improvement of flexural properties of polypropylene (PP) could be achieved by blending it with a stiffer polymer like poly(ethylene terephthalate) (PET). The main problem is the compatibilization between a saturated, apolar structure with a polar polyester. Copolymers of glycidyl methacrylate (GMA) and 2-ethylhexyl acrylate (EHA) were prepared, characterized and used as compatibilizers in PP/PET (70/30 wt%) blends at different feed ratios. The effects of compatibilization of these polymers were analyzed by SEM, which shows reduction of the size of PET granules, and by TGA, with an increase in the thermal stability of the compatibilized blends. Thermal properties corresponding to melting and crystallization events were also changed by the introduction of the compatibilizers. The DMTA shows that the T_g of the PET domain is affected by compatibilization, contrary to the T_g of PP domain. The compatibilization efficiency was further confirmed by an increase in flexural strain at flexural strength (ε_{FM}).

Keywords Compatibilization · Polypropylene · Poly(ethylene terephthalate) · Polymeric blends · Glycidyl methacrylate

Introduction

Over the years, several blends of polymers have received scientific attention. Effective polymeric blends could be the key to achieve not only materials with high industrial value and improved performance, but also to develop materials incorporating post-consumer plastics [1–3].

Polypropylene (PP) is one of the most commonly consumed polyolefins in the world, due to its versatility, relatively low-price, good flexibility, easy processability and excellent barrier properties [4, 5]. However, PP is susceptible to oxidation, accelerated both by heat and UV radiation, which influences its mechanical properties [6–8]. It is well-established that a straightforward way to upgrade the properties of PP, particularly the mechanical performance, and broaden its field of applications, is to successfully blend it with other polymers particularly with PET [4, 9]. Generally, blends of PP with PET and other polymers are typically hampered by incompatibility, as the result of negligible entropy of mixing for long chain molecular interactions [2, 10].

Studies on blends of PP and PET, generally showed a clear two-phase morphology, proving the immiscibility behavior of these two polymers. This fact leads to a lack of interfacial adhesion between the two phases and is detrimental for the mechanical performance, as the strong material requires that the applied load is evenly distributed through both phases. The morphology of the dispersed phase is highly dependent upon the processing conditions, volume fraction of components and the quality of the interactions between the two polymers [11–13]. The use of compatibilizers as the third component of the blend has had a beneficial impact of mitigating the differences in the chemical nature and polarity between these two polymers. Generally, compatibilizers are copolymers with structures that interact/react with the components of the blend improving the interfacial adhesion between the immiscible polymer phases [10–12, 14]. In the case of PP-PET mixtures, a common solution is to use functional polyolefins for interchain polymer reactions with the terminal hydroxyl and carboxyl of the polyester [15, 16]. Studies showed that effective compatibilization could be obtained from an efficient dispersion of a compatibilizer able to enhance the inter-diffusivity of the PP and PET chains. This has been achieved through the presence of both apolar groups, such as alkyl chains, able to interact with PP

Electronic supplementary material The online version of this article (https://doi.org/10.1007/s10965-019-1784-7) contains supplementary material, which is available to authorized users.

✉ Arménio C. Serra
armenio.serra@gmail.com

[1] CEMMPRE, Department of Chemical Engineering, University of Coimbra, Pólo II, Pinhal de Marrocos, 3030-790 Coimbra, Portugal

and reactive groups able to react with PET terminals [17, 18]. The most commonly described reactive groups for such in situ compatibilizers are maleic anhydride [5, 11, 18–22] and epoxide [2, 15, 22], with varying degrees of success. Compatibilizers containing an epoxide functionality, providing reactivity with both carboxyl and hydroxyl groups of PET, bear a higher reactivity than the ones with maleic anhydride and have been considered more effective [1, 17]. Different commercial solutions with epoxide functionalities have also been studied as potential PP/PET compatibilizers [1, 14, 17].

Such epoxide functional polymers could be introduced with other monomers (such as ethyl acrylates), resulting in the production of epoxide functional copolymers which can be used for different applications such as coatings and adhesives [23–26]. The copolymerization of 2-ethylhexyl acrylate (EHA) with glycidyl methacrylate (GMA), has improved the mechanical stability, tensile strength and the elasticity of the material [23]. To the best of our knowledge, no research has been done on the usage of poly (glycidyl methacrylate)-*random*-poly(2-ethylhexyl acrylate) (PGMA-*co*-PEHA) copolymers as a potential compatibilizer for PP/PET blends.

In this work, a straightforward method is described to synthesize two PGMA-*co*-PEHA copolymers with significantly different PGMA/PEHA molar ratios: 70/30 and 15/85. Their physicochemical properties were determined, focusing mainly on ^{1}H NMR, FTIR and TGA techniques. Due to their intrinsic properties, the PGMA-*co*-PEHA copolymers were studied, for the first time, as potential compatibilizers for PP/PET (70/30 wt%) blends. A series of PP/PET blends with varying amounts of compatibilizer were studied in terms of microstructure, thermal and mechanical properties. Throughout the work, the mechanical properties of the PP/PET blends with the novel compatibilizers have been compared with those containing a commercial compatibilizer.

Experimental

The materials used in this study were ethanol (EtOH, 100%, José Manuel Gomes dos Santos, Lda., Odivelas, Portugal), polyvinylpyrrolidone (PVP, wt 10,000, Sigma-Aldrich, China), 2,2′ – Azobis (2-methylpropionitrile) (AIBN, 98%, Aldrich, France) and alumina (basic, Fisher Scientific) were used as received. GMA (97%, Acros, Netherlands) and EHA (98%, Alfa Aeser, Germany) were passed through a sand/alumina column before use to remove the radical inhibitor. Polypropylene ISPLEN PB 110 H2E (PP, melt mass-flow rate (230 °C; 2.16 kg) of 0.3 g/10 min, density of 0.905 g/cm^3), poly(ethylene terephthalate) SELENIS INFINITE S82 (PET, intrinsic viscosity of 0.82 dl/g, melt point of 255 °C) and a commercial compatibilizer bearing epoxy functional groups (CC), were provided by Componit Lda. (Portugal), and dried in an oven at 50 °C for a minimum of 12 h prior to use.

Synthesis of the PGMA-co-PEHA copolymers

The synthesis of the PGMA-*co*-PEHA copolymers was carried out through the described method for PGMA in the presence of polyvinylpyrrolidone (PVP) (see Scheme 1) [27]. PVP (2.9 g, 0.3 mmol) was dissolved in EtOH (62 mL) in a round bottomed flask equipped with a magnetic stirrer. AIBN (0.4 g, 2.4 mmol) was then added to the flask followed by GMA (20.8 g, 0.2 mol) and EHA (9.7 g, 48.9 mmol). The mixture was then purged with N_2 for 10 min. The flask was equipped with a condenser, the temperature raised to 70 °C and the reaction allowed to proceed for 24 h. The final reaction mixture was washed with hexane and the polymer recovered by solvent removal under reduced pressure. In order to determine the relative amount of monomer incorporation into the copolymer, ^{1}H nuclear magnetic resonance (NMR) of the product was performed. Size exclusion chromatography (SEC), Fourier transform infrared (FTIR), thermogravimetric analysis (TGA) and dynamic mechanical thermal analysis (DMTA) were used to characterize the materials. A similar procedure was followed with a different GMA/EHA molar feed ratio, 25/75, to attain a PGMA-*co*-PEHA copolymer bearing less amount of epoxide groups (Table 1).

Typical processing conditions of the PP/PET-based formulations

Prior to melt blending PP, PET and commercial compatibilizer (CC) were dried in an oven at 50 °C for a minimum of 12 h to

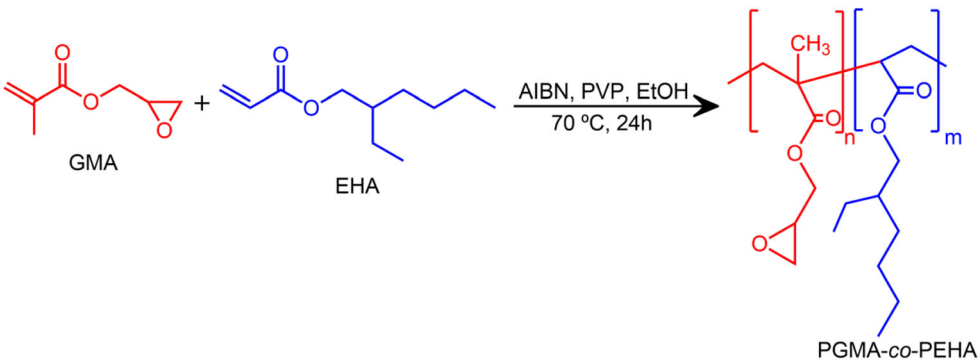

Scheme 1 Reaction conditions for the synthesis of PGMA-*co*-PEHA copolymers

Table 1 Summary of the reaction conditions used in the synthesis of the PGMA-*co*-PEHA copolymers

Entry	Sample Code	Molar feed ratio* (%)		V_{EtOH} (mL)
		GMA	EHA	
#1	Reaction 1	75	25	62
#2	Reaction 2	25	75	112

*$[EHA + GMA]_0/[PVP]_0/[AIBN]_0$ = 1/0.15/1.25 M ratio

remove any residual moisture from the samples. The PGMA-*co*-PEHA were stored under reduced pressure prior to use. After drying, different PP/PET (70/30 wt% ratio) blends were prepared with the use of compatibilizer at different feed ratios: 0 wt%, 1 wt%, 2.5 wt% and 5 wt% (Table 2). The blends were prepared in a two-roll mill bender (Thermo Scientific – Haake polylab), at 240 °C and 60 rpm for 10 min. After blending, the materials were pressed (> 1 t) in a hydraulic press (Carver 2101, 100–400 °C, 230 V, Fred S. Carver Inc., USA) at 250 °C, for 10 min, to obtain 2 mm thick plaques. The final blend plaques were cut into pieces with a CNC mini milling machine for various characterization techniques. For notation purposes, throughout the work GE, or $G_{70}E_{30}$, refers to the synthesized PGMA-*co*-PEHA bearing a PGMA/PEHA molar ratio of 70/30 and EG, or $E_{85}G_{15}$, to the one bearing a PGMA/PEHA molar ratio of 15/85.

Physico-chemical and mechanical characterization

^{1}H NMR spectra of PMGA-*co*-PEHA copolymers were recorded on a 400 MHz NMR spectrometer (Brucker Avance III XXMHz) using $CDCl_3$ as solvent, at room temperature. Tetramethylsilane (TMS) was used as the internal reference.

Size exclusion chromatography (SEC) was used to analyze the polymer mass distribution of final PGMA-*co*-PEHA copolymers. The chromatographic parameters of the samples were determined using a Viscotek (Viscotek TDAmax) size exclusion chromatograph (SEC) equipped with an on-line degasser, a differential viscometer (DV), right-angle laser-light scattering (RALLS) (Viscotek); low-angle laser-light scattering (LALLS) (Viscotek), and refractive index (RI) detectors. The column set consisted of a Viscotek Tguard column (8 μm), one Viscotek T2000 column (6 μm), one Viscotek T3000 column (6 μm), and one Viscotek LT4000L column (7 μm). An HPLC dual piston pump was set at a flow rate of 1 mL/min. The analyses were carried out at 30 °C using an Elder CH-150 heater. Before the injection (100 μL), the samples were filtered through a polytetrafluoroethylene (PTFE) membrane with 0.2 μm pore. The system was calibrated with narrow polystyrene (PS) standards. The number-average molecular weight (M_n^{SEC}) and dispersity ($Đ$) of synthesized polymers were determined by conventional calibration using OmniSEC software version: 4.6.1.354 (Malvern Instrument Ltd., Worcestershire, UK).

Table 2 Summary of the feed ratios of PP, PET and compatibilizers (GE, EG or CC) used in the studied formulations

Entry	Formulation	PP (wt%)	PET (wt%)	Compatibilizer (wt%)		
				GE	EG	CC
#1	PP/PET/0	70.00	30.00	0.00	0.00	0.00
#2	PP/PET/GE1	69.30	29.70	1.00	–	–
#3	PP/PET/GE2.5	68.25	29.25	2.50	–	–
#4	PP/PET/GE5	66.50	28.50	5.00	–	–
#5	PP/PET/EG1	69.30	29.70	–	1.00	–
#6	PP/PET/EG2.5	68.25	29.25	–	2.50	–
#7	PP/PET/EG5	66.50	28.50	–	5.00	–
#8	PP/PET/CC1	69.30	29.70	–	–	1.00
#9	PP/PET/CC2.5	68.25	29.25	–	–	2.50
#10	PP/PET/CC5	66.50	28.50	–	–	5.00

Fourier transform infrared (FTIR) spectra were obtained in the 4000–600 cm^{-1} range at room temperature using an Agilent Technologies Carey 630 spectrometer, equipped with a Golden Gate Single Reflection Diamond ATR. Data collection was performed with 4 cm^{-1} spectral resolution and 64 accumulations.

Thermogravimetric analysis (TGA) was carried out using a Q500 thermogravimetric analyzer (TA Instruments, USA) with a thermobalance sensitivity of 0.1 μg, to characterize the thermal stability of the materials. The equipment was calibrated within a temperature interval ranging from 25 °C to 1000 °C, at a heating rate of 10 °C.min^{-1}, running tin and lead as melting standards. The samples were analyzed using open alumina crucibles, in the temperature range of 25 °C to 600 °C and at a heating rate of 10 °C.min^{-1}, under dry nitrogen purge flow of 100 mL.min^{-1}.

The differential scanning calorimetry (DSC) measurements were performed in a Q100 DSC model (TA Instruments, USA), equipped with a RCS90 cooling unit, in order to determine the characteristic temperatures of the materials. The heat flow and the heat capacity were calibrated at 5 °C.min^{-1} using indium and sapphire standards, respectively. The samples were analyzed in aluminum pans with a loosely placed ordinary aluminum lid. All scans were done in a dry nitrogen environment with a purge flow of 50 mL.min^{-1} and at a heating/cooling rate of 10 °C.min^{-1} ranging from −80 °C to 300 °C. DSC analysis for all the samples were performed in three consecutive runs of heating-cooling-heating, starting from heating the samples from room temperature to 300 °C, followed by cooling to −80 °C and heating again to 300 °C. Values for ΔH_c and ΔH_m were normalized by the weight percentage of the corresponding polymers.

The viscoelastic properties of the studied materials were measured by dynamic mechanical thermal analysis (DMTA) with a Tritec 2000 DMA (Triton Technology, Ltd., UK). The geometry of the assay was conditioned by the sample type: the PGMA-

co-PEHA copolymers were analyzed in the single cantilever bending geometry using stainless steel material pockets, and the PP/PET-based blends in the dual cantilever bending geometry. All DMTA measurements were carried out in a − 150 °C to 200 °C temperature range, at frequencies of 1 and 10 Hz, using a heating rate of 2 °C.min^{-1}. The glass transition temperature (T_g) of the studied materials was determined from the maximum of the tan δ curve, at 1 Hz. The reported data corresponds to the average of the results of 3 individual samples.

To investigate the dispersion of the PET in the polymeric blend the fracture surfaces were analyzed by scanning electron microscopy (SEM). The specimens were frozen in liquid nitrogen prior to fracture to diminish the risk of plastic deformation. The fracture surfaces were coated with gold and analyzed in a Field Emission Scanning Electron Microscope (FESEM), ZEISS MERLIN Compact/VPCompact, Gemini II.

The flexural properties of composites were determined using SHIMADZU AG-IS testing machine at a temperature of 23 ± 2 °C. For flexural tests (ASTM D790), a three-point loading system was used, and the support span length was adjusted to 32 mm, radius support was adjusted to 2 mm, radius nose was adjusted to 5 mm and the crosshead speed was 1 mm/min. The reported result is the average of five individual measurements.

Tensile mechanical tests were carried out on a Chatillon TCD100 mechanical tester equipped with a 5 kN load cell. The dumbbell shaped samples were pulled at a rate of 1 mm.min-1 until fracture. The Young's modulus was calculated from the initial slope of the curve after removing the toe region. The values were averaged by analysis of five valid tests.

Results and discussion

Synthesis and characterization of the PGMA-co-PEHA copolymers

The approach used for the synthesis of PGMA-*co*-PEHA copolymer is based on the free radical copolymerization of GMA and EHA using PVP as stabilizer (Scheme 1). The use of these conditions is expected to minimize the risk of epoxide opening during the copolymerization [27].

As previously mentioned, two initial molar feed ratios of GMA/EHA were used to attain different PGMA-*co*-PEHA copolymers (Table 1). The structural characterization of final PGMA-*co*-PEHA copolymers was performed by ^{1}H NMR. The characteristic signals of the double bond on both GMA and EHA were residual at the end of reactions indicating a very high monomer conversion. Hence, structural characterization of both copolymers was performed on purified samples. Figure 1 presents the ^{1}H NMR spectrum of a sample of PGMA-*co*-PEHA copolymer with a GMA/EHA feed ratio of 75/25, representing the characteristic proton chemical shifts in the copolymers.

The ^{1}H NMR spectrum of a PGMA-*co*-PEHA copolymer with a GMA/EHA feed ratio of 75/25 (GE, Fig. 1) shows the characteristics signals of both GMA and EHA incorporated into the polymeric chain. The characteristic signals due to the presence of EHA are as follows: **(k)** at 0.9 ppm corresponding to the six protons of -C**H**$_3$ groups; **(j)** at 1.3 ppm attributed to the eight protons of -C**H**$_2$- groups; **(g)** and **(i)** in the range of 1.6–2 ppm correspond to three protons of -C**H**$_2$- and C**H** groups; **(h)** at 3.7 ppm is due to two protons of -OC**H**$_2$- group [24, 28]. Furthermore, the resonance peaks of the GMA domain can be found at: **(b)** at 0.9 ppm due to the protons of -C**H**$_3$ group; **(c)** attributed to the protons of the –OC**H**$_2$- group and has two contributions in the range of 4.5–3.6 ppm; **(e)** and **(d)** in the range of 2.5–3.4 ppm, are the characteristic signals of epoxide groups [24]. Similar findings were found in the ^{1}H NMR spectrum of EG (Fig. S 1). The ^{1}H NMR spectra also allowed the determination of the exact ratio between the epoxide and the alkyl portion incorporated in the polymers. The determination of the PGMA/PEHA ratio was possible due to the ratio between the integration of **(c)** and **(c), (h)** peaks via eqs. 1 and 2.

$$F_{PGMA}\ (\%) = \frac{A}{0.5B + A} \times 100 \quad (1)$$

$$F_{PEHA}\ (\%) = \frac{0.5B}{0.5B + A} \times 100 \quad (2)$$

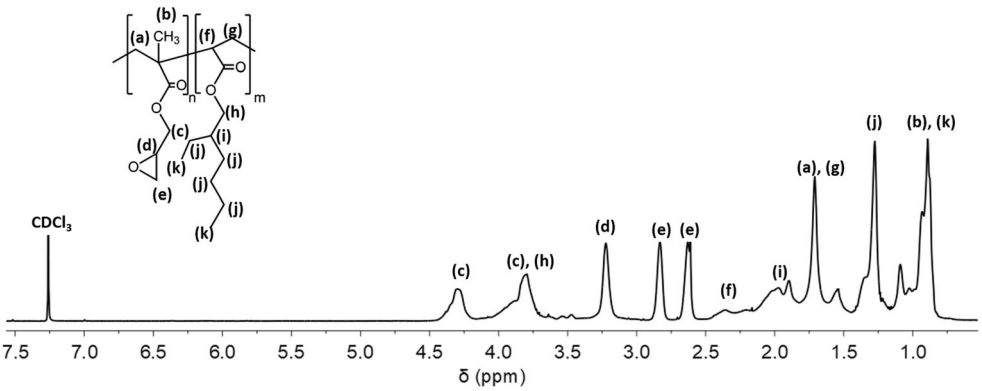

Fig. 1 400 MHz ^{1}H NMR spectrum, in $CDCl_3$, of a purified PGMA-*co*-PEHA copolymer (reaction conditions: $[GMA]_0/[EHA]_0/[AIBN]_0/[PVP]_0 = 75/25/1.25/0.15$, $V_{EtOH} = 62$ mL)

where A is the total integrated peak area, from 4.5–4.2 ppm, attributed to half of the protons of the –OC**H**$_2$- group in GMA (isolated contribution of 1 H of **(c)** protons), and B (contribution of the two protons of the -OC**H**$_2$- group in EHA (peak **(h)**) is the result of the total integrated peak area from 4.1–3.6 ppm (peak **(c), (h)**) minus the total integrated peak area from 4.5–4.2 ppm (isolated contribution of 1 H of **(c)** protons). With these calculations, it was determined that sample GE had a PGMA/PEHA molar ratio of 70/30, and compatibilizer EG a 15/85 PGMA/PEHA molar ratio.

Table 3 presents the general properties of both the synthesized PGMA-*co*-PEHA copolymers.

As shown in Table 3, the molar ratios between the GMA and EHA segments differed relatively to the feed, especially for the EG sample. This is due to the different reactivity of the two comonomers [24, 26, 29].

Purified samples from both copolymers were analyzed by FTIR spectroscopy to assess the presence of the epoxide moieties. Figure 2 depicts the FTIR spectra of copolymers in the range of 500 to 3500 cm^{-1}. The presence of the epoxide signals is expected in the region between 1050 and 800 cm^{-1}, detailed in the inlet box (Fig. 2b).

The Fig. 2 shows three bands at 845 cm^{-1}, 905 cm^{-1} and 990 cm^{-1} that can be attributed to the epoxide group PGMA-*co*-PEHA samples [30, 31]. This is a strong indication that with this reaction system the integrity of the epoxide is maintained during the polymerization. Furthermore, a slight intensity difference of epoxide bands is observed for the two copolymers, being lower for the EG sample as expected.

To be potential compatibilizers, it is crucial that the PGMA-*co*-PEHA copolymers are thermally stable at the processing temperature of PP-PET (i. e. 240-250 °C). The thermal properties of the copolymers were investigated by TGA (Fig. 3 and Table 4). Figure 3 displays the recorded weight loss and the first derivative curves for the studied copolymers.

As shown in Fig. 3, both copolymers are thermally stable at the temperature of future processing (i.e. 240–250 °C), being this temperature well below the temperature corresponding to 5% of mass loss ($T_{5\%}$, Table 4). In fact, these copolymers could withstand temperatures above 315 °C with a weight loss of under 10% ($T_{10\%}$, Table 4). This residual mass loss registered at lower temperatures could be ascribed to the degradation of oligomers and copolymers of low molecular weights.

Taking a closer look at the weight loss profiles from the PGMA-*co*-PEHA copolymers, it should be noticed that the EG sample presented a slightly faster degradation profile, most likely due to its lower molecular weight (Table 3). Furthermore, the EG thermogravimetric plots only exhibit one evident degradation stage, with a temperature of maximal rate of decomposition of 395.7 °C (T_{max}, Table 4). For the copolymer bearing a higher content of epoxy moieties, GE, there is a deviation of the maximum weight loss to lower temperatures, 371.8 °C. Moreover, in this sample a second degradation stage is evident by the presence of a shoulder on the first derivative plot, with a maximum registered at 402.3 °C. The data from the thermogravimetric plots of both GE and EG is consistent with the reports from Dubois et al. [26] for PEHA-*co*-PGMA copolymers bearing varying amounts of EHA in the copolymer structure. As the rates of EHA decreased in the polymeric structure the temperature of maximal degradation rate shifted to lower temperatures and a shoulder appeared at higher temperatures. This shift in T_{max} could be ascribed to the increasing content of epoxy moieties, as it is reported that the PGMA homopolymer has a distinct two-stage degradation profile.

Samples were also analyzed by DSC, however no clear thermal transitions were observed, and the copolymers were classified as amorphous, as expected due to their random structure. Hence, on both samples the glass transition temperature (T_g) was determined by DMTA (Table 4). The Tan δ profile at 1 and 10 Hz is represented in Fig. S 2. As anticipated, the copolymer with a higher GMA content (70/30 PGMA/PEHA molar ratio, sample GE) has a glass transition temperature significantly higher ($T_g = 50.5$ °C) than the copolymer bearing a higher ratio of alkyl chains (15/85 PGMA/PEHA molar ratio, sample EG, $T_g = -32.4$ °C). These findings further support the claim that the glass transition temperature of PGMA-*co*-PEHA copolymers could be tuned by varying the PGMA/PEHA molar ratio in the polymers' architecture [24].

Preparation and characterization of the PP/PET-based blends

The compatibilizing effect of different GMA containing polymers on PP/PET blends has been reported. Champagne et al.

Table 3 General properties of the PGMA-*co*-PEHA copolymers

Sample code	Molar feed ratio (%)		Molar ratio in the copolymer (%)*		$M_n \times 10^{-3}$	M_w/M_n
	GMA	EHA	PGMA	PEHA		
GE	75	25	70	30	40.67	3.04
EG	25	75	15	85	7.59	3.43

*Determined by ^{1}H NMR spectroscopy

Determined by SEC

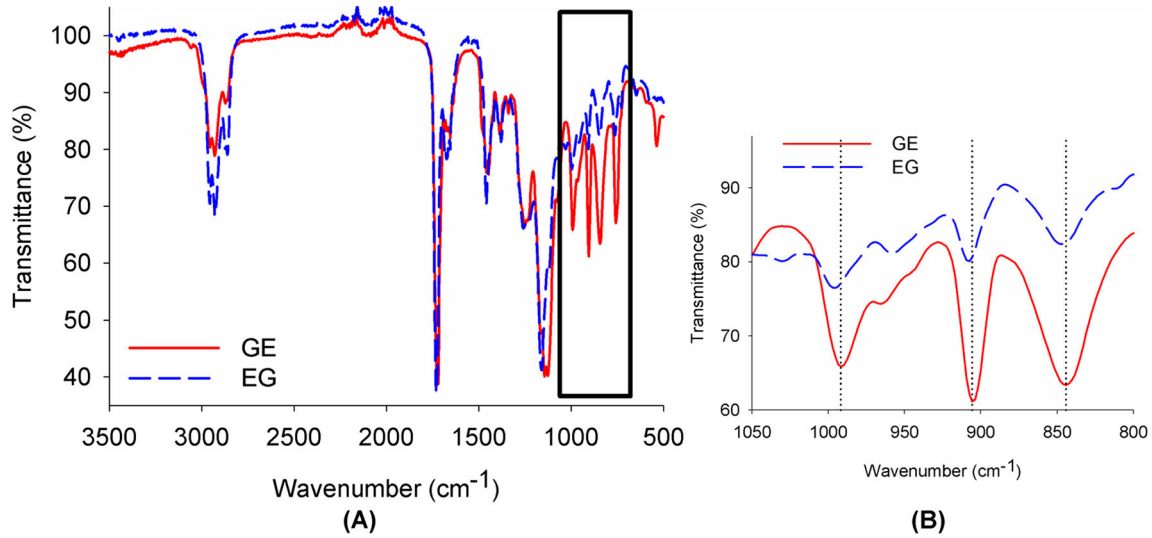

Fig. 2 FTIR spectra of samples from the PGMA-*co*-PEHA copolymers with different PGMA/PEHA molar ratios: 70/30 ($G_{70}E_{30}$, blue dashed traces) and 15/85 ($E_{85}G_{15}$, red traces). The inlet box, expanded in (**b**), magnifies the spectrum from 1050 to 800 cm^{-1} to clarify the epoxide bands

reported that the usage of PP-g-GMA as a PP/PET compatibilizer increased the elongation at break up to 20-fold in PET-rich blends [2]. The work of Jarestani et al. reported an enhanced compatibility effect of *n*-buyl-acrylate-gycidyl-methacrylate-ethylene both in the microstructure and mechanical behavior of PP/PET blends [17]. This enhanced compatibility of epoxy-containing compatibilizers was also reported by Rageart et al. where both a polyolefin-g-GMA and especially a (styrene ethylene butylene styrene)-*g*-GMA (SEBS-*g*-GMA) showed a beneficial effect on toughness, morphology and rheology [1]. Enhanced interactions between the PP and PET phase were also reported to be induced by SEBS-*g*-GMA by Heino et al [14]. The synthesized PGMA-*co*-PEHA copolymers, (GE) and (EG) were used as compatibilizers for PP/PET blends with a unique feed ratio of 70/30 wt%. The epoxy moieties in the copolymers could react with PET end groups (COOH or OH) during the melt mixing (Scheme 2) while the pendent alkyl chains of the PEHA segments should be able to interact with the PP domains [2, 17, 19].

Aiming to assess the influence that the amount of compatibilizer has on the final properties of PP/PET blends, different compatibilizer ratios were used, as described in Table 2: 0, 1, 2.5 and 5 wt%. A commercial compatibilizer (CC) was used throughout as a reference. The performance of the studied PP/PET blends was assessed in terms of processing torque, physicochemical properties (FTIR, TGA, DSC and DMTA) and mechanical properties, evaluated in terms of flexural assays.

Each of the studied PP/PET-based blends, (with adequate quantities of PP, PET and compatibilizer; Table 2) was processed in a polymer mixer at 240 °C, 60 rpm and for 10 min. During the processing stage the evolution of torque overtime was considered. For all the blends a slight decrease of torque

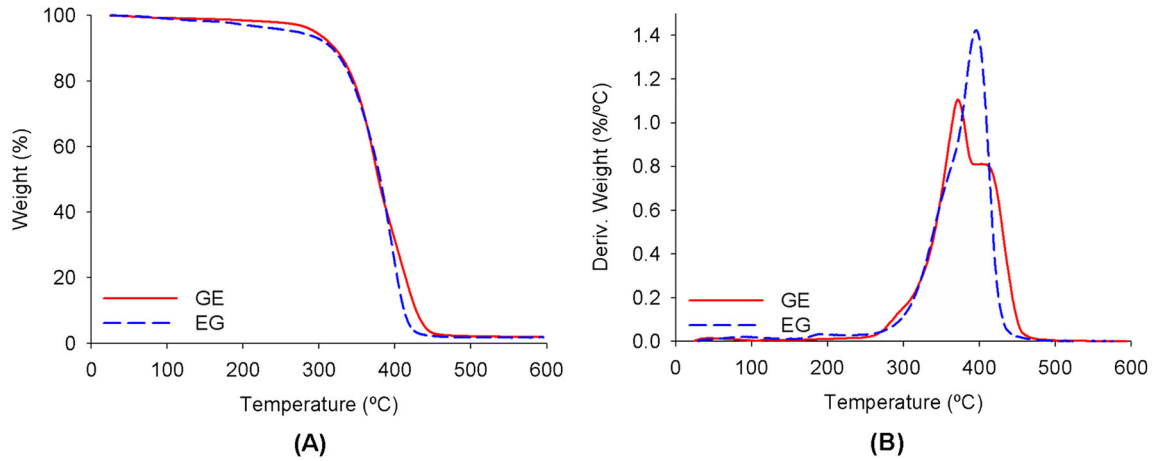

Fig. 3 Weight loss **(a)** and first derivative **(b)** of the TGA curves obtained from samples of the studied PGMA-*co*-PEHA copolymers with different PGMA/PEHA molar ratios: 70/30 ($G_{70}E_{30}$, blue dashed traces) and 15/85 ($E_{85}G_{15}$, red traces)

Table 4 Thermal properties determined for the PGMA-*co*-PEHA copolymers

Sample code	TGA			DMTA
	$T_{5\%}$ (°C)	$T_{10\%}$ (°C)	T_{max} (°C)	T_g (°C)
GE	292.4	319.0	371.8 / 402.3*	50.5
EG	267.0	315.8	395.7	−32.4

*Maximum of the shoulder visible in the first derivative curve for the GE sample

values with time is observed probably due to degradation of PET of PP chains and decreasing in the molecular weight [32, 33]. For the PP/PET blend without the addition of any compatibilizer (Fig. S 3), it is possible to see that the addition of PET to the melted PP initially increases the processing torque to over 20 Nm. This value rapidly decreases to ca. 5 Nm in the first 2 min of processing indicating the melt mixing of both components. During the remaining processing time, the torque of the PP/PET blend continued to show a gradual decrease until it stabilized at 3.0 Nm (Table S 1).

With the addition of the different compatibilizers, at different feed ratios, the final torque after the same process of stabilization is different. Figure 4 compares the processing torque vs. time curves of the studied blends, with and without the addition of the different compatibilizers, upon stabilization. The torque values of the different blends during the 10 min processing can be consulted in Table S 1.

The results from Fig. 4 show that the addition of a compatibilizer typically caused an increase in torque upon stabilization. This increase was especially evident for the blend containing 2.5 wt% of GE (5.0 Nm; Table S 1) and 5 wt% of the commercial compatibilizer (CC) (4.2 Nm). This increase in viscosity, which results in higher torque values, could be explained by the occurrence of reactions capable of increasing the molecular weight of the blend [30]. However, for the PP/PET blends compatibilized with the PGMA-*co*-PEHA copolymer with higher ratio of PEHA (sample EG), no significant increase in processing torque is observed. In fact, when 5 wt% of EG was used as a compatibilizer the torque was lower (2.5 Nm) than when no compatibilizer was used. This might be explained by an increase in fluidity of the blend due to a higher amount of alkyl chains able to interact with the PP domain of the blend causing some plasticizing effect over the mixture.

Physicochemical properties of the PP/PET-based blends

FTIR

The influence of the different compatibilizers on the blend was also assessed by FITR (Fig. S 5 – Fig. S 7). With the addition of the different epoxy-containing compatibilizers, it is expected to see some changes on characteristic epoxide peaks after blending (Fig. 5). For comparison purposes a physical mixture

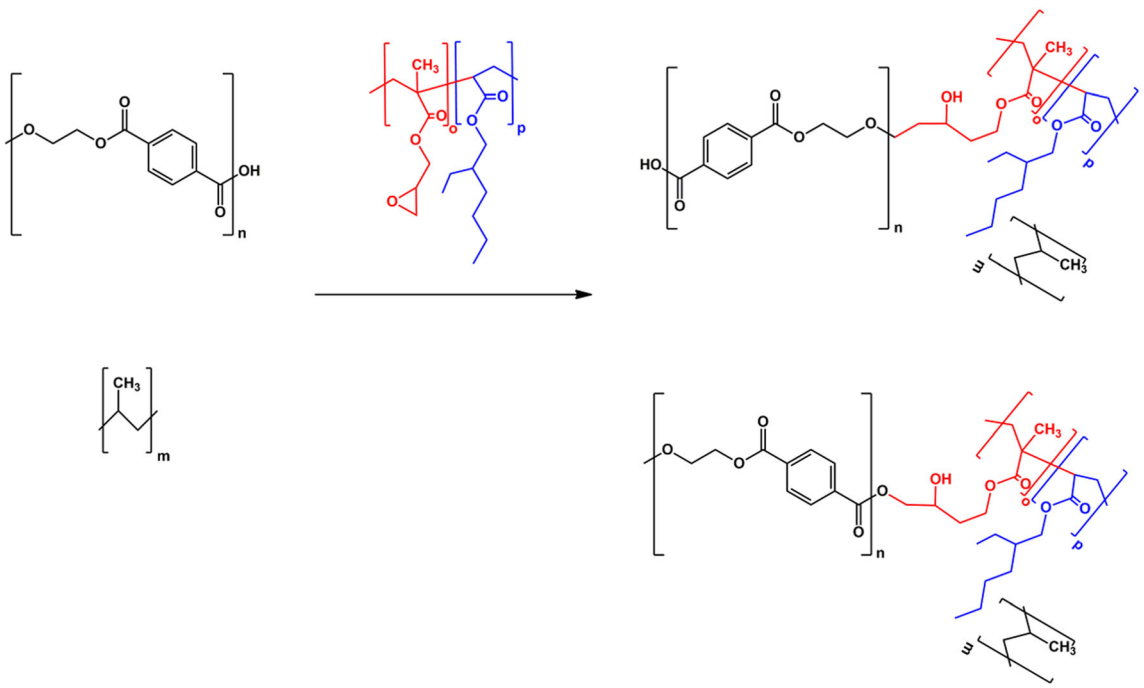

Scheme 2 Representation of the possible reactions and interactions between the PGMA-*co*-PEHA copolymers and both PP and PET. Emphasis on the possible reactions between the terminal groups of PET and the epoxy groups of the compatibilizer

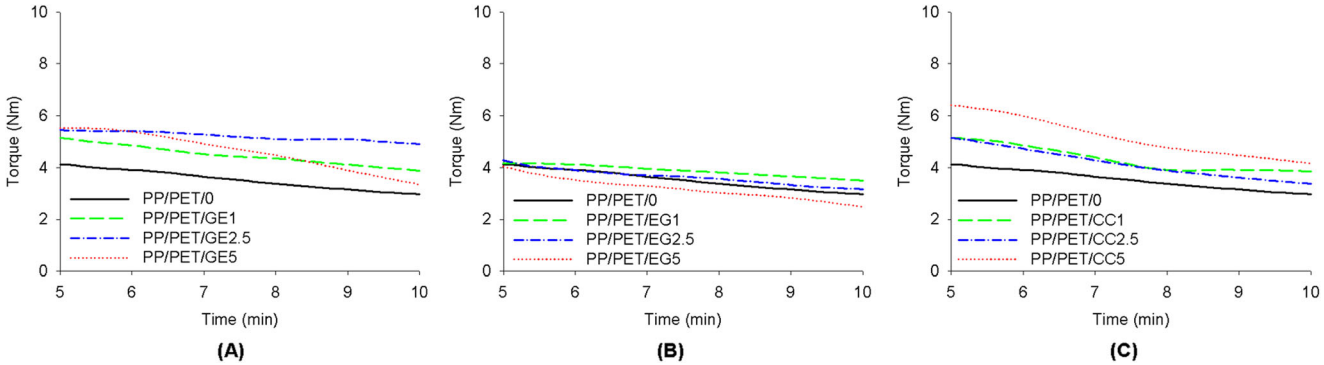

Fig. 4 Torque vs time curves for the studied PP/PET blends with and without varying amounts of compatibilizer after 5 min of mixture: **a** $G_{70}E_{30}$, **b** $E_{85}G_{15}$ and **c** CC

of PP/PET and 5% of GE without melt blending was also analyzed.

From Fig. 5 it is possible to see that the blend of PET/PP presents bands with absorptions close to the values corresponding to the vibrations of the epoxide groups (845 cm^{-1}, 905 cm^{-1} and 990 cm^{-1}) [30, 31, 34–36]. In the case of the physical mixture (red dashed line) the relative intensity of the bands is different compared with the bands observed after melting blending process (red line). Particularly the band assigned to the asymmetric stretching (905 cm^{-1}) [37, 38] is greatly reduced, indicating that a reaction occurred between the epoxy moieties of the copolymer and the PET domain.

Microstructure

The impact on the microstructure of the different compatibilized PP/PET blends, was assessed via SEM images taken from the cryofractured surfaces of the materials. The images of the PP/PET blends compatibilized with different amounts of GE, and the non-compatibilized (PP/PET/0) sample are showed in Fig. 6. Similar images taken from materials compatibilized with either EG or CC can be viewed in Fig. S 8 and Fig. S 9, respectively. In Table S 2 the average diameters of the PET domain determined for the studied materials are reported.

Significant changes in the morphology of the PET domain with varying amounts of compatibilizer GE are visible in Fig. 6. In the sample with no compatibilizer (Fig. 6a) it is possible to see large spheres, corresponding to the PET domain, dispersed in the PP matrix [1, 14]. It is also possible to see the craters left behind in the matrix through the removal of the PET spheres during the cryofracture process. Both the spheres and the craters have diameters up to 30 μm. Interestingly, the addition of 1 wt% of (PP/PET/GE1) was enough to alter the morphology of the PET domain from spheres to tubular structures with a diameter of ca. 5 μm. Nonetheless, smaller spheres (ca. 3 μm) were also visible in this sample. With increasing compatibilizer ratios (Fig. 6c, d), these tubular structures were no longer visible, the PET domain having recovered its initial conformation of sphere-like structures, but with smaller diameters. Similar findings were found for the samples where EG was used as the compatibilizer (Fig. S 8). Increasing the amount of this compatibilizer content from 2.5 wt% to 5 wt% didn't appear to influence the average diameter of the PET spheres, the slight differences in size being within the standard deviation (Table S 2). By SEM analysis, the compatibilizer that had the most efficient effect

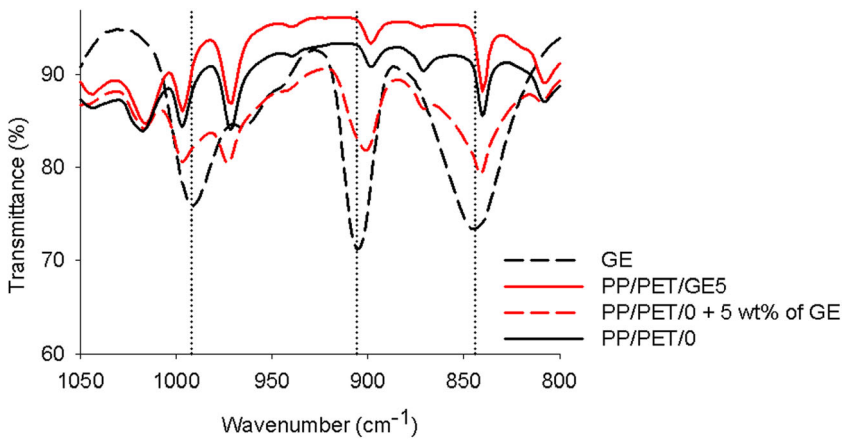

Fig. 5 Comparison between the FTIR spectra in the characteristic epoxide region of a $G_{70}E_{30}$ sample (black dashed trace), a PP/PET/GE5 sample (Entry #4, Table 2) (red trace), a PP/PET/0 sample (Entry #1, Table 2) (black trace) and of a physical mixture of PP/PET sample with 5 wt% of $G_{70}E_{30}$ (red dashed trace). Vertical dotted lines correspond to the characteristic epoxy peaks at 990 cm^{-1}, 905 cm^{-1} and 845 cm^{-1}

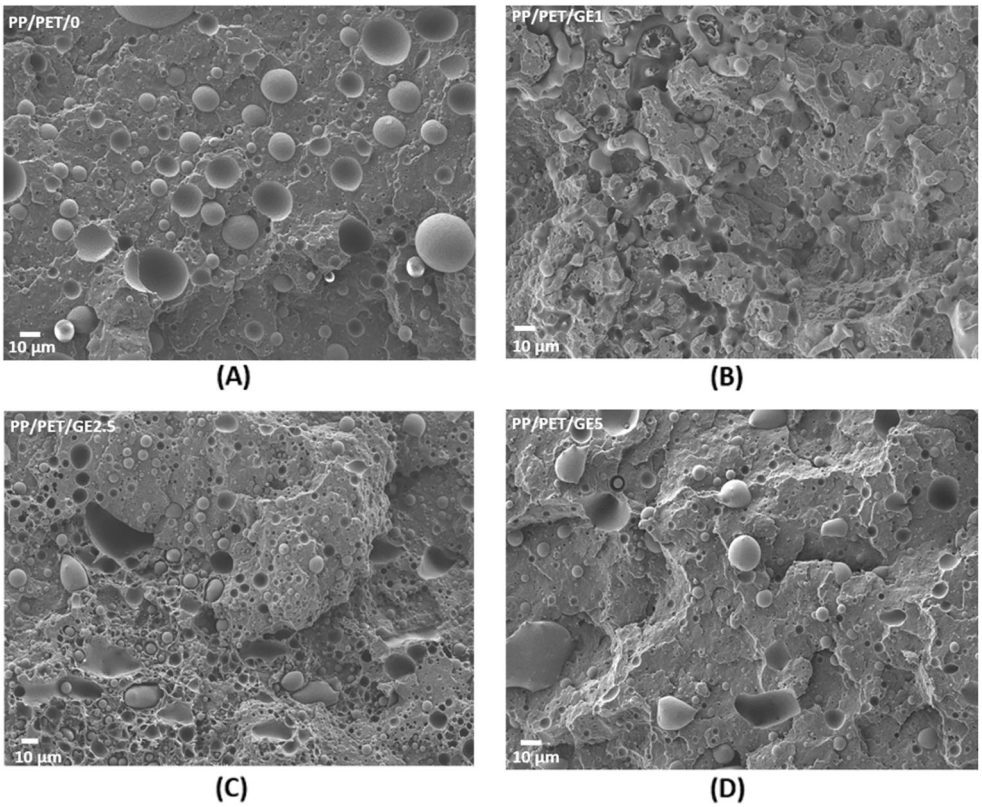

Fig. 6 SEM micrographs of the cryofractured surface of different PP/PET blends: **a** PP/PET/0, **b** PP/PET/GE1, **c** PP/PET/GE2.5 and **d** PP/PET/GE5. Scale bar 10 µm

on the size of PET particles was the commercially available compatibilizer, CC (Fig. S 9 and Table S2).

Thermal characterization

The thermal stability of the studied blends, with and without the addition of varying amounts of compatibilizer, was assessed by TGA. In Fig. 7 are represented the thermogravimetric plots of the PP/PET blends compatibilized with varying amounts of GE. The TGA profiles of the blends compatibilized with either EG or CC, due to the similarity with PP/PET/GE based materials are shown in supplementary information (Fig. S 10). Table 5 summarizes the characteristic temperatures taken from the thermogravimetric plots of the studied blends.

The results from the thermogravimetric curves (Fig. 7 and Fig. S 10) show that the addition of the compatibilizer had a beneficial effect on the thermal stability, when compared with the non-compatibilized material (PP/PET, entry #1 of Table 5). From the TGA profiles, one broad peak corresponding to a single step process of degradation is observed for a maximum mass loss for all PP/PET blends. The addition of compatibilizer to the PP/PET-based material causes a significant shift in the TGA curves to higher temperatures, increasing the degradation temperatures at both 5% and 10% weight loss ($T_{5\%}$ and $T_{10\%}$), with a direct impact on the temperature of maximal rate of decomposition (T_{max}, Table 5). This increase in thermal stability with the addition of the compatibilizers could be ascribed to the formation of chemical bonds between PET chains and compatibilizer. It has been described that the existence of carboxylic end groups in PET has a direct effect on its thermal and hydrolytic stability [4, 39–41]. Hence, the observed higher stability could be due to the decrease of the amount of free carboxylic groups by reaction with epoxide groups of the compatibilizer. With slight deviations, the results seem to point to indicate a ratio of 2.5 wt% of compatibilizer in the blend originate blends with the highest thermal stability. The lower stability of samples with 5% compatibilizers could be due to the presence of a greater amount of this material with lower stability (see Fig. 3).

The influence of the synthesized compatibilizers on the crystallization and melting behavior of both the PP and PET domains in each blend was determined by DSC. The crystallization of both domains was observable in the cooling scans, being the melting processes observable in the second heating scans. In Fig. 8 the DSC scans for blends compatibilized with varying amounts of either GE or EG are presented. The scans from blends compatibilized with CC can be found in Fig. S 12. The relevant thermal data for all the samples is summarized in Table 6.

The DSC thermograms for the second heating of neat PP and neat PET can be seen in Fig. S 11. From the thermogram of the neat PET it was possible to distinguish a clear exothermic peak at ca. 160 °C, coinciding with the endothermic peak

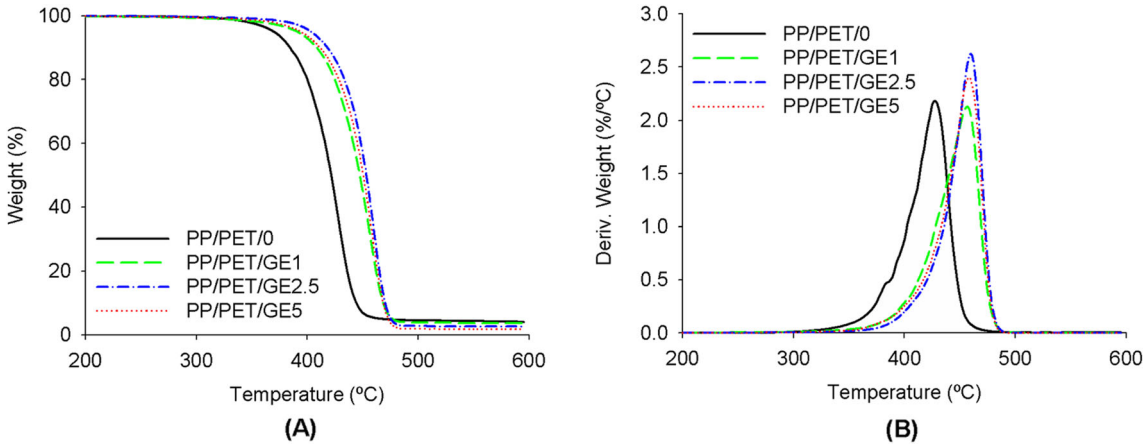

Fig. 7 Weight loss (%; **(a)**) and first derivative (%/°C; **(b)**) of the thermogravimetric plots of samples from the studied PP/PET blends with varying amounts of GE: 0 wt% (black line), 1 wt% (green dashed line), 2.5 wt% (blue dash-dotted line) and 5 wt% (red dotted line)

present in the thermogram of the neat PP, and an endothermic peak at ca. 245 °C. These two endothermic peaks, evident in the thermogram of the non-compatibilized blend (Fig. S 11) are thus attributed to the melting temperatures of the PP (T_m^{PP}) and PET (T_m^{PET}) domain. It has been reported that the crystallization of the PP region and temperature of crystallization (T_c) of PP in PP/PET blends increases with increasing PET concentration; PET acts as a heterogeneous nucleation agent for the growth of PP crystallites [42]. Due to the overlap between the exothermic peak found for neat PET and the endothermic peak of neat PP, the study of the temperatures of crystallization (T_c) of PET was carried out in the cooling scans.

From the cooling scans, Fig. 8a, c and Fig. S 12 (A), it is possible to distinguish two evident events that correspond to the crystallization of the PET and PP. The first, sharper and at *ca* 120 °C, is attributed to the crystallization of the PP domain, being the second peak at *ca* 200 °C, derived from the crystallization of the PET domain. With respect to PP crystallization, in the presence of compatibilizers (GE and EG) the T_c of all blends are at lower temperatures (Table 6). Comparing the effect of the two compatibilizers, the one with lower T_c values is the copolymer EG. The reason for this behavior is linked to the higher interaction of the ethyl hexyl chains of EG with polypropylene domains. This event is not so significant with copolymer GE with a lower ratio of these alkyl chains [42–44]. Similar findings were observed for the commercial compatibilizer (Fig. S 12 (A)). Moreover, the ΔH_c^{PP} of compatibilized samples is higher than that of the non-compatibilized blend for the case of 2.5 and 5 wt% addition of either EG or GE copolymers. For 1 wt% of the compatibilizer, the ΔH_c^{PP} decreases. The broader peaks observed in compatibilized samples, particularly in the case of EG and CC containing blends, could be due to a slower crystallization process induced by the greater affinity of this compatibilizer to the PP domain [45].

For the PET crystallization process, it is interesting to notice that the use of 1 wt% of compatibilizer caused an increase in its crystallization temperature in relation to the non-compatibilized sample, without significant enthalpy changes. With higher compatibilizer content (2.5 and 5 wt%), this transition typically shifts to lower temperatures with lower enthalpies. This indicates a higher degree of compatibilization of PET due to reactions with epoxide groups. The amorphous nature of compatibilizer linked to PET domains may decrease the crystallinity levels by reducing the diffusional process during crystallization [18, 44].

Analysis of the 2nd heating run shows two endothermic peaks, Fig. 8b, d and Fig. S 12 (B), associated with the melting temperatures of the PP (T_m^{PP}, at ca. 160 °C) and the PET (T_m^{PET}, at ca. 240 °C) domains. For PP domains the results showed no major changes compared with the non-compatibilized samples. The exception is the compatibilizer EG in 5% (Fig. 8d red trace) which shows a lower T_m (158 °C). The presence of alkyl chains in this amorphous compatibilizer hinders the formation of native PP crystals leading to the appearance of imperfect PP crystals [46]. In

Table 5 Characteristic temperatures of the studied blends taken from the TGA

Entry	Formulation	$T_{5\%}$ (°C)	$T_{10\%}$ (°C)	T_{max} (°C)
#1	PP/PET/0	370.96	384.74	427.39
#2	PP/PET/GE1	390.40	408.84	456.60
#3	PP/PET/GE2.5	404.68	418.68	459.85
#4	PP/PET/GE5	395.35	411.80	458.12
#5	PP/PET/EG1	385.58	404.26	453.82
#6	PP/PET/EG2.5	392.38	407.70	455.67
#7	PP/PET/EG5	375.04	397.60	456.28
#8	PP/PET/CC1	397.11	413.67	457.10
#9	PP/PET/CC2.5	405.46	417.59	455.08
#10	PP/PET/CC5	390.32	408.72	448.23

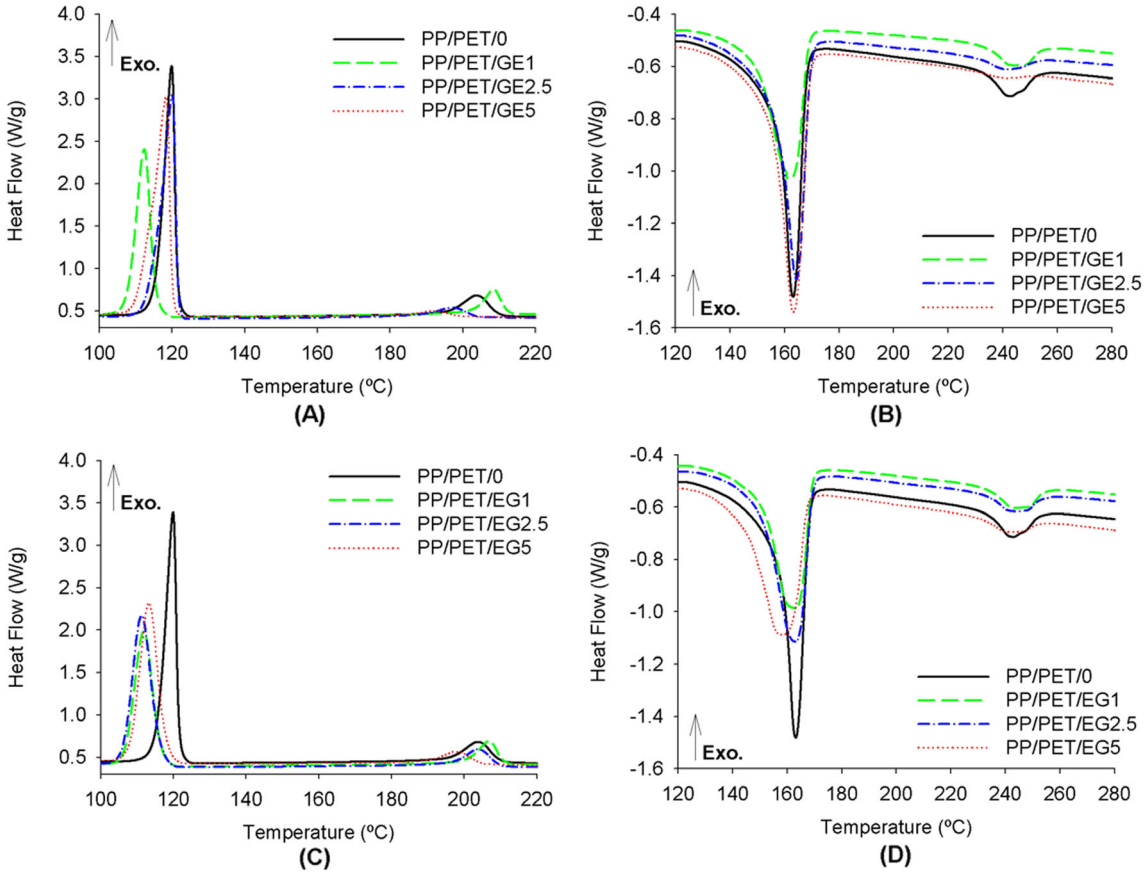

Fig. 8 DSC of the studied PP/PET blends compatibilized with varying amounts of $G_{70}E_{30}$ (top) and $E_{85}G_{15}$ (bottom) during the cooling (**(a)** and **(c)**) and heating (**(b)** and **(d)**) scans

relation to PET domain, the presence of compatibilizers does not significantly change the melting temperatures. However, major differences are seen in the ΔH_m values which decrease with increasing compatibilizer content, especially for blends with GE and EG at 5%, (Fig. 8b, d). This is due to reactions of PET with compatibilizers that transform crystalline PET into a more amorphous material.

Thermomechanical characterization: DMTA

DMTA analysis of PET/PP blends are not commonly found in literature [4, 14]. This technique enabled the measurement of the stiffness and damping of the blended materials [47, 48]. The elastic response is represented by the storage modulus (E'), whereas the viscous response is related to its loss

Table 6 Summary of the characteristic data from the DSC analysis of the studied PP/PET (70/30 wt%) blends with varying amounts of the different compatibilizers

Entry	Formulation	T_c^{PP} (°C)	T_C^{PET} (°C)	ΔH_c^{PP} (J/g)	ΔH_c^{PET} (J/g)	T_m^{PP} (°C)	T_m^{PET} (°C)	ΔH_m^{PP} (J/g)	ΔH_m^{PET} (J/g)
#1	PP/PET/0	119.93	203.64	100.64	41.87	163.05	242.86	82.64	25.60
#2	PP/PET/GE1	112.36	208.37	88.69	38.11	160.91	244.17	68.21	19.93
#3	PP/PET/GE2.5	120.10	197.06	114.23	20.21	164.30	241.58	87.56	10.36
#4	PP/PET/GE5	118.34	191.66	128.47	12.25	163.15	--*	103.19	--*
#5	PP/PET/EG1	111.88	206.80	84.56	38.92	163.31	244.18	67.84	22.53
#6	PP/PET/EG2.5	111.26	203.66	105.04	35.52	163.18	243.61	79.85	16.85
#7	PP/PET/EG5	113.26	197.84	110.93	27.12	157.97	242.20	82.92	14.42
#8	PP/PET/CC1	111.33	208.05	83.20	42.05	163.20	245.12	62.63	25.56
#9	PP/PET/CC2.5	112.11	196.06	97.86	37.88	164.15	244.37	77.98	23.35
#10	PP/PET/CC5	110.48	193.75	94.32	35.93	163.15	247.77	75.08	22.35

*Transition was not visible

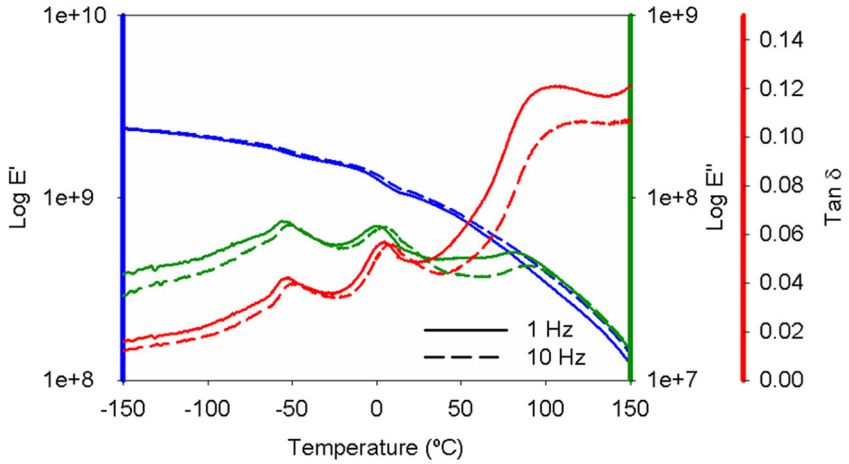

Fig. 9 DMTA curves of a non-compatibilized PP/PET (70/30 wt%) sample at frequencies 1 Hz and 10 Hz

modulus (E"). From the ratio between the moduli it is possible to determine the Tan δ (damping), which measures the samples' capacity to dissipate energy [49]. The DMTA traces of the non-compatibilized sample (PP/PET 70/30 wt%), at frequencies 1 Hz and 10 Hz, are presented in Fig. 9. The DMTA traces of the blends with compatibilizers are presented in the supporting information (Fig. S 12 - Fig. S 17), and the relevant thermomechanical parameters are reported in Table S 3 and summarized in Fig. 10.

In a DMTA analysis the temperature at which the Tan δ peak reaches its maximum, at 1 Hz, is attributed to the glass transition temperature (T_g) of the material. From Fig. 9 it is possible to observe that the non-compatibilized sample (PP/PET/0) exhibits three frequency sensitive events. It is known from literature that isotactic PP typically has two T_g, being the first (−52 °C) due to the presence of a small portion of atactic chains and is dependent upon the molecular weight of the sample. The second (4 °C), is due to the amorphous region of the material, rich in isotactic chains [50]. For comparison purposes, the tan δ profile of the DMTA curves of a neat PP sample (Fig. S 13) show the presence of these two T_gs. Above this temperature, the material markedly loses its mechanical properties and softens, affecting the tan δ profile in the temperature range at which the T_g of the PET domain is expected (104 °C, compare with Fig. S 14)).

The impact of the compatibilization process on the storage (E') and loss (E") moduli, at 25 °C (room temperature) can be viewed in Fig. 10.

A close analysis of Fig. 10 shows that the compatibilization process generally increases both the storage (E') and the loss (E") moduli in relation to the non-compatibilized sample. The use of higher amounts of compatibilizers does not induce significant improvements in these two parameters. Interestingly, GE and EG copolymers show a general increase of these two parameters compared with the commercial compatibilizer.

DMTA is a highly reliable technique for the determination of the glass transition temperature of the polymers in the blend, as this transition is hardly seen in DSC analysis. Data regarding the T_g of the PP domain in the blend showed no relevant changes that could be assigned to the compatibilization (Table S 3). However, the compatibilization had a clear impact on the glass transition ascribed to the PET domain (Fig. 11). This was especially evident for blends with 2.5 wt% of compatibilizers where the T_g^{PET} was ca. 10 °C lower than that of the non-compatibilized blend. This lowering, corresponding to values towards those of the T_g^{PP}

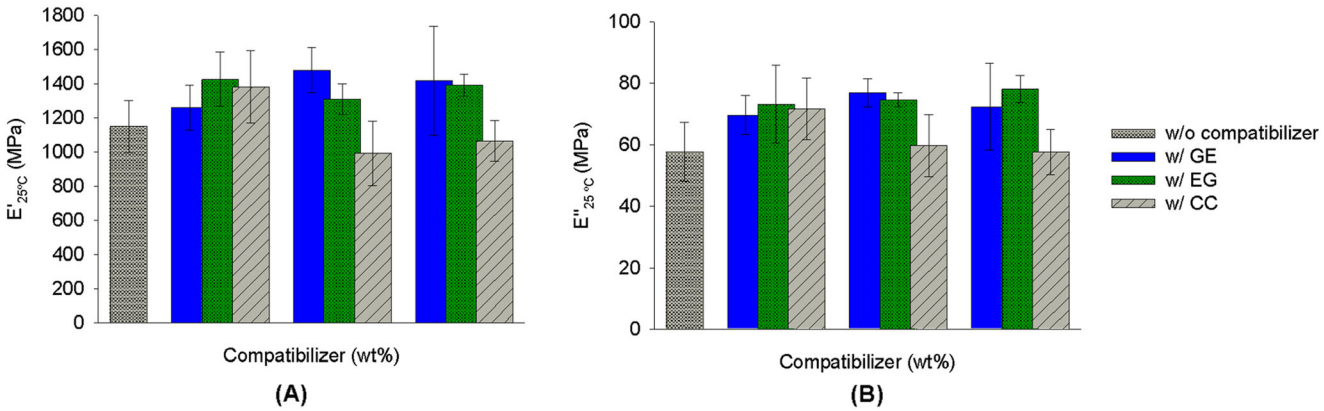

Fig. 10 Influence of the compatibilizer (wt%) on thermomechanical properties of the PP/PET (70/30 wt%) blends in terms of the storage (E', **(a)**) and loss (E", **(b)**) moduli, at 25 °C

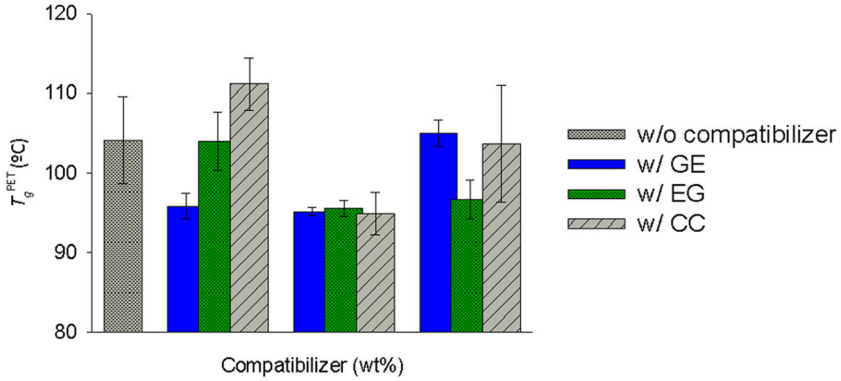

Fig. 11 Influence of the compatibilizer (wt%) on thermomechanical properties of the studied blends in terms of the glass transition of the PET domain (T_g^{PET})

(Table S 3), is a clear evidence of the enhancement of interactions between the two domains that is more relevant with this amount of compatibilizers [4, 14, 41, 43].

Mechanical properties

Tensile tests of PP/PET blends are more described than flexural tests with or without the presence of a compatibilizer. One of the major limitations of a non-compatibilized PP/PET blend is that, although the addition of PET to a PP matrix typically increases the strength of the material, its ability to withstand load without failure and toughness, is low. Typically, non-compatibilized PP/PET materials have low elongations at break [11, 13]. The mechanical behavior of an incompatible polyester/polyolefin blend is strongly dependent upon the type of compatibilizer used [11, 13, 43, 51]. The PP/PET-based materials in compatibilized and non-compatibilized forms were subjected to tensile tests (Fig. S18). In the presence of compatibilizer (namely at 5% concentration) there is a gain in the Young modulus and no major loss with respect to the elongation at break. Among tested compatibilizers the synthesized GMA copolymers present better performances.

In the case of flexural assays, Fig. 12 summarizes the results obtained in terms of flexural modulus (E), flexural

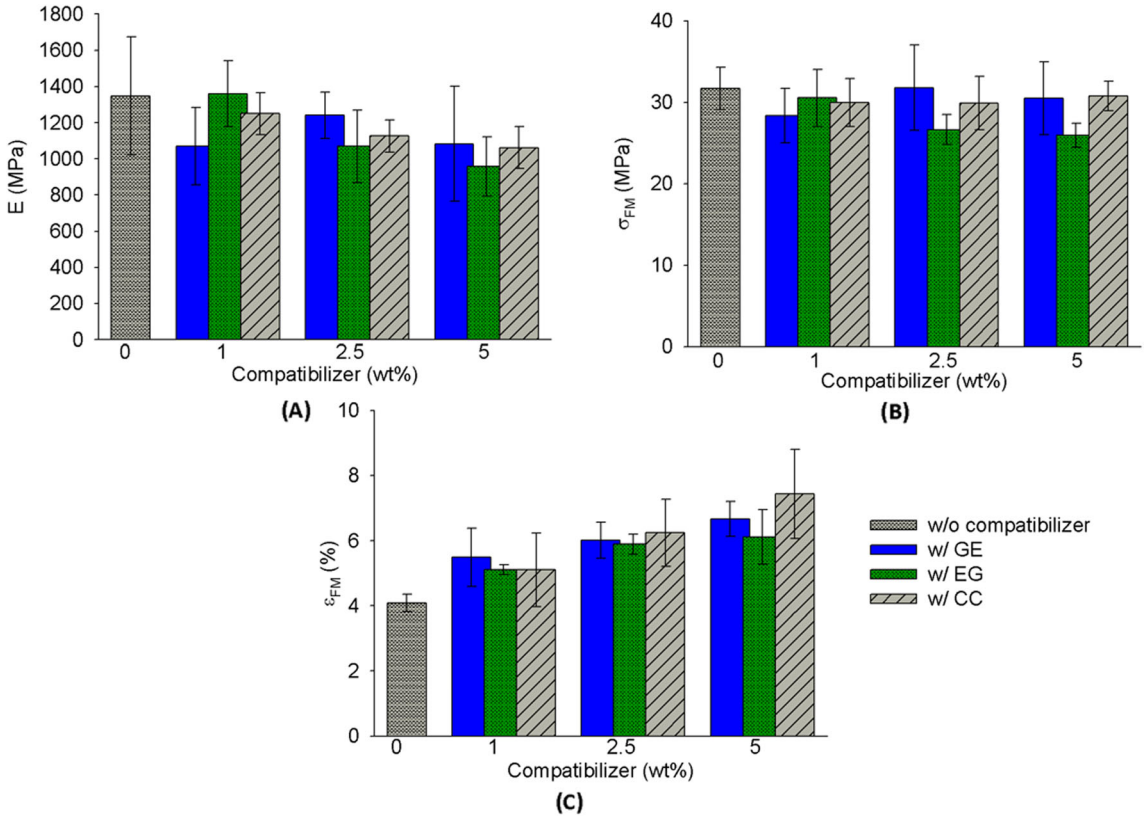

Fig. 12 Influence of the amount of compatibilizer (wt%) on the flexural properties of the studied blends in terms of **(a)** flexural modulus, E, **(b)** flexural strength, σ_{FM}, and **(c)** flexural strain at flexural strength, ε_{FM}

strength (σ_{FM}) and flexural strain at flexural strength (ε_{FM}). Detailed results can be found in Table S 4.

The results from Fig. 12 show that the addition of the different compatibilizers at different ratios did not result in the increase of the stiffness or strength of the materials as reported using other compatibilizers [5, 9, 14, 19]. In fact, the compatibilized materials typically displayed lower flexural modulus (E, Fig. 12a). The impact in the flexural strength (σ_{FM}, Fig. 12b) was not as significant, as nearly all materials were able to maintain the high strength displayed by the non-compatibilized PP/PET material. However, the compatibilized samples have higher flexural strain at flexural strength (ε_{FM}, Fig. 12c) (up to 50%) than the sample without compatibilizer (PP/PET/0), which a clear indication of an improvement in interface adhesion caused by compatibilization [43]. Moreover, this parameter increases with increasing compatibilizer content. In sum, results show that the addition of compatibilizers drastically increase the ε_{FM}, and thus the toughness of the blend. At the same time, no significant changes are found in the strength of the different materials.

Conclusions

Copolymers of glycidyl methacrylate (GMA) and 2-ethylhexyl acrylate (EHA) were successfully prepared and characterized. The copolymers, with significantly different PGMA/PEHA molar ratios (70/30 and 15/85) in its structure and an amorphous nature, were evaluated as compatibilizers in PP/PET (70/30 wt%) blends at different feed ratios. The compatibilization led to significant changes in the morphology of the PET domain, particularly to a decrease in the size of PET spheres disperse in the PP matrix. Compatibilized blends also displayed a higher thermal stability than non-compatibilized samples. From DSC analysis it is concluded that the temperature of PP crystallization decreases in the presence of compatibilizers, especially in the presence of a higher amount of ethyl hexyl chains. PET crystallization process is also changed depending on the amount of compatibilizer used due to the reactions with the epoxy group. DMTA experiments showed an increase in both the storage (E') and the loss (E") moduli in relation to the non-compatibilized sample. In relation to T_g of the polymers in the blends only the T_g of PET shows an evident impact being 10 °C lower than the non-compatibilized blend. The success of the compatibilization was further supported by the significant increase in flexural strain at flexural strength (ε_{FM}) in relation to the non-compatibilized blend, which is a strong indication of good interfacial adhesion between each domains of the blend.

In sum, the combined effect of the epoxy pendent groups and the pendent ethyl hexyl chains present in the PGMA-*co*-PEHA copolymers allow these materials to interact with both components of the PP/PET blends. The properties of the final material could be tuned by varying the PGMA/PEHA molar ratio in the compatibilizer. The results from this work show that blends compatibilized with the PGMA-*co*-PEHA copolymers had competitive performances with commercially available samples, which expands the field of applications for these polymeric structures.

Acknowledgments The authors acknowledge project Flexmodulo, POCI-01-0247-FEDER-003362 for financial support. The ^{1}H NMR data was collected at the UC-NMR facility which is supported in part by FEDER –European Regional Development Fund through the COMPETE Programme (Operational Programme for Competitiveness) and by National Funds through FCT – Fundação para a Ciência e a Tecnologia (Portuguese Foundation for Science and Technology) through grants REEQ/481/QUI/2006, RECI/QEQ-QFI/0168/2012, CENTRO-07-CT62-FEDER-002012, and Rede Nacional de Ressonância Magnética Nuclear (RNRMN).

References

1. Van Bruggen EPA, Koster RP, Picken SJ, Ragaert K (2016) Influence of processing parameters and composition on the effective Compatibilization of polypropylene–poly(ethylene terephthalate) blends. Int Polym Process 31(2):179–187
2. Champagne MF, Huneault MA, Roux C, Peyrel W (1999) Reactive compatibilization of polypropylene/polyethylene terephthalate blends. Polym Eng Sci 39(6):976–984
3. Gnatowski A, Koszkul J (2005) Investigations of the influence of compatibilizer and filler type on the properties of chosen polymer blends. J Mater Process Technol 162–163:52–58
4. Inuwa IM, Hassan A, Samsudin SA, Haafiz MKM, Jawaid M (2017) Interface modification of compatibilized polyethylene terephthalate/polypropylene blends: effect of compatibilization on thermomechanical properties and thermal stability. J Vinyl Addit Technol 23(1):45–54
5. Abdul Razak NC, Inuwa IM, Hassan A, Samsudin SA (2013) Effects of compatibilizers on mechanical properties of PET/PP blend. Compos Interfaces 20(7):507–515
6. Oswald HJ, Turi E (1965) The deterioration of polypropylene by oxidative degradation. Polym Eng Sci 5(3):152–158
7. Maier C, Calafut T (1998) Polypropylene: the definitive User's guide and Databook. William Andrew Inc, New York
8. Schoolenberg GE, Vink P (1991) Ultra-violet degradation of polypropylene: 1. Degradation profile and thickness of the embrittled surface layer. Polymer 32(3):432–437
9. Xanthos M, Young MW, Biesenberger JA (1990) Polypropylene/polyethylene terephthalate blends compatibilized through functionalization. Polym Eng Sci 30(6):355–365
10. White JL, Yang J (2008) In: Domasius N., thein K. (eds) polyolefin blends. Wiley, New York
11. Cheung MK, Chan D (1999) Mechanical and rheological properties of poly(ethylene terephthalate)/ polypropylene blends. Polym Int 43(3):281–287
12. Barlow JW, Paul DR (1984) Mechanical compatibilization of immiscible blends. Polym Eng Sci 24(8):525–534
13. Santos P, Pezzin SH (2003) Mechanical properties of polypropylene reinforced with recycled-PET fibres. J Mater Process Technol 143–144:517–520
14. Heino M, Kirjava J, Hietaoja P, Seppa J (1997) Compatibilization of polyethylene terephthalate / polypropylene blends with styrene – ethylene / butylene – styrene (SEBS) block copolymers. J Appl Polym Sci 65(2):241–249

15. Moad G (1999) The synthesis of polyolefin graft copolymers by reactive extrusion. Prog Polym Sci 24(1):81–142
16. Ciardelli F, Aglietto M, Coltelli M, Passaglia E, Giacomo R, Coiai S (2004) In: Ciardelli F., Penczek S. (eds) Modification and Blending of Synthetic and Natural Macromolecules. Kluwer Academic Publ, Pisa
17. Amanizadeh F, Naderi A, Jarestani Y, Kaptan N (2014) Rheologically determined phase behavior and miscibility of reactively compatibilized poly(ethylene terephthalate)/polypropylene blends. Polym Bull 71(6):1315–1329
18. Papadopoulou CP, Kalfoglou NK (2000) Comparison of compatibilizer effectiveness for PET/PP blends: their mechanical, thermal and morphology characterization. Polymer 41(7):2543–2555
19. Pang YX, Jia DM, Hu HJ, Hourston DJ, Song M (2000) Effects of a compatibilizing agent on the morphology, interface and mechanical behaviour of polypropylene / poly (ethylene terephthalate) blends. Polymer 41(1):357–365
20. Chiu HT, Hsiao YK (2006) Compatibilization of of poly (ethylene terephthalate)/ polypropylene blends with maleic anhydride grafted polyethylene-octene elastomer. J Polym Res 13(2):153–160
21. Wang Y, Run M (2009) Non-isothermal crystallization kinetic and compatibility of PTT/PP blends by using maleic anhydride grafted polypropylene as compatibilizer. J Polym Res 16:725–737
22. Jazani OM, Rastin H, Formela K, Hejna A, Shahbazi M, Farkiani B, Saeb MR (2017) An investigation on the role of GMA grafting degree on the efficiency of PET/PP-g-GMA reactive blending: morphology and mechanical properties. Polym Bull 74:4483–4497. https://doi.org/10.1007/s00289-017-1962-x
23. Jerenec S, Šimić M, Savnik A, Podgornik A, Kolar M, Turnšek M, Krajnc P (2014) Glycidyl methacrylate and ethylhexyl acrylate based polyHIPE monoliths: morphological, mechanical and chromatographic properties. React Funct Polym 78:32–37
24. Haloi DJ, Roy S, Singha NK (2009) Copper catalyzed atom transfer radical copolymerization of glycidyl methacrylate and 2-ethylhexyl acrylate. J Polym Sci Part A Polym Chem 47:6536–6533
25. Khelifa F, Habibi Y, Bénard F, Dubois P (2012) Effect of cellulosic nanowhiskers on the performances of epoxidized acrylic copolymers. J Mater Chem 22:20520–20528
26. Khelifa F, Druart ME, Habibi Y, Bénard F, Leclère P, Olivier M, Dubois P (2013) Sol–gel incorporation of silica nanofillers for tuning the anti-corrosion protection of acrylate-based coatings. Prog Org Coatings 76(5):900–911
27. Daniel H, Pavlo S (2000) Reactive poly(glycidyl methacrylate) microspheres prepared by dispersion polymerization. J Polym Sci Part A Polym Chem 38(21):3855–3863
28. Vidts KRM, Dervaux B, Du Prez FE (2006) Block, blocky gradient and random copolymers of 2-ethylhexyl acrylate and acrylic acid by atom transfer radical polymerization. Polymer 47(17):6028–6037
29. Dhal PK, Ramakrishna MS, Babu GN (1982) Copolymerization of glycidyl methacrylate with alkyl acrylate monomers. J Polym Sci Part A Polym Chem 20(6):1581–1585
30. Tsai CH, Chang FC (1996) Polymer blends of PBT and PP Compatibilized by ethylene-co-glycidyl methacrylate copolymers. J Appl Polym Sci 61(2):321–332
31. Souza AMC, Caldeira CB (2015) An investigation on recycled PET/PP and recycled PET/PP-EP compatibilized blends: Rheological,morphological, and mechanical properties. J App Polym Sci 132:41892
32. Wang X, Yu W, Nie Q, Guo Y, Du J (2011) A real-time study on the evolution of the degradation of polypropylene during mixing process. J App Polym Sci 121:1220–1243
33. Duarte IS, Tavares AA, Lima PS, Andrade DLACS, Carvalho LH, Canedo EL, Silva SML (2016) Chain extension of virgin and recycled poly(ethylene terephthalate): effect of processing conditions and reprocessing. Polym Degrad Stab 124:26–34
34. Luongo JP (1960) Infrared study of polypropylene. J Appl Polym Sci 3(9):302–309
35. Miyake A (1959) The infrared spectrum of polyethylene terephthalate. I the effect of crystallization. J Polym Sci 38(134):479–495
36. Daniels WW, Kitson RE (1958) Infrared spectroscopy of polyethylene terephthalate. J Polym Sci 33(126):161–170
37. Erol I, Poyraz B, Koroglu MA, Cifci C (2009) Copolymerization of 2-methyl-*N*-1,3-thiazole-2-ylacrilamide with glycidyl methacrylate:synthesis, characterization, reactivity ratios and biological activity. J Polym Res 16(1):19–28
38. Kalfoglou NK, Skafidas DS, Kallitsis J, Lambert JC, Stappen LV (1995) Comparison of compatibilizer effectiveness for PET/HDPE blends. Polymer 26(23):4453–4462
39. Berti C, Bonora V, Colonna M, Lotti N, Sisti L (2003) Effect of carboxyl end groups content on the thermal and electrical properties of poly(propylene terephthalate). Eur Polym J 39(8):1595–1601
40. Jabarin SA, Lofgren EA (1984) Thermal stability of polyethylene terephthalate. Polym Eng Sci 24(13):1056–1063
41. Al-AbdulRazzak S, Jabarin SA (2002) Processing characteristics of poly(ethylene terephthalate): hydrolytic and thermal degradation. Polym Int 51(2):164–173
42. Zhu Y, Liang C, Bo Y (2015) Non-isothermal crystallization behavior of compatibilized polypropylene / recycled polyethylene terephthalate blends. J Therm Anal Calorim 119(3):2005–2013
43. Zhu Y, Liang C, Bo Y, Xu S (2015) Compatibilization of polypropylene/recycled polyethylene terephthalate blends with maleic anhydride grafted polypropylene in the presence of diallyl phthalate. J Polym Res 22:35
44. Inoya H, Leong YW, Klinklai W, Thumsorn S, Makata Y, Hamada H (2011) Compatibilization of recycled poly(ethylene terephthalate) and polypropylene blends: effect of polypropylene molecular weight on homogeneity and compatibility. J Appl Polym Sci 124(5):3947–3955
45. Kunimune N, Yamada K, Leong YW, Thumsorn S, Hamada H (2010) Influence of the reactive processing of recycled poly(ethylene terephthalate)/poly(ethylene-co-glycidyl methacrylate) blends. J Appl Polym Sci 120(1):50–55
46. Jayanarayanan K, Thomas S, Joseph K (2011) In situ microfibrillar blends and composites of polypropylene and poly (ethylene terephthalate): morphology and thermal properties. J Polym Res 18(1):1–11
47. Coelho JFJ, Carreira M, Popov AV, Gonçalves PMOF, Gil MH (2006) Thermal and mechanical characterization of poly(vinyl chloride)-b-poly(butyl acrylate)-b-poly(vinyl chloride) obtained by single electron transfer – degenerative chain transfer living radical polymerization in water. Eur Polym J 42(10):2313–2319
48. Coelho JFJ, Carreira M, Gonçalves PMOF, Popov AV, Gil MH (2006) Processability and characterization of poly(vinyl chloride)-b-poly(n-butyl acrylate)-b-poly(vinyl chloride) prepared by living radical polymerization of vinyl chloride. Comparison with a flexible commercial resin formulation prepared with PVC and dioctyl phthalate. J Vinyl Addit Technol 12(4):156–165
49. Schlesing W, Buhk M, Osterhold M (2004) Dynamic mechanical analysis in coatings industry. Prog Org Coatings 49(3):197–208
50. Yasaku W, Yasuko H, Ryuji S (1968) Glass transition and relaxation in the amorphous phase of isotactic polypropylene. J Polym Sci Part C Polym Symp 23(2):583–595
51. Inoya H, Leong YW, Klinklai W, Takai Y, Hamada H (2012) Compatibilization of recycled poly(ethylene terephthalate) and polypropylene blends: effect of compatibilization on blend toughness, dispersion of minor phase and thermal stability. J Appl Polym Sci 124:5260–5269